2. J. F. B. Mitchell, T. C. Johns, J. M. Gregory, S. F. B. Tett, *Nature* **376**, 501 (1995).
3. R. J. Charlson *et al.*, *Science* **255**, 423 (1992).
4. J. T. Kiehl and B. P. Briegleb [*ibid.* **260**, 311 (1993)] and J. Hansen, M. Sato, and R. Ruedy [*Atmos. Res.* **37**, 175 (1995)] demonstrated that the direct radiative influence of sulfate aerosols is far too small to correct the simulations; it would have to be indirect, through their ability to alter cloud properties. The amplitude of the latter is highly speculative; compare (*1*) and A. Jones, L. Roberts, A. Slingo, *Nature* **370**, 450 (1994). Hansen, Sato, and Ruedy (in preparation) argue that the direct effect of the aerosols may be entirely canceled by a semidirect effect in which heating due to aerosol absorption reduces low cloud cover. Some inconsistencies of the aerosol cooling hypothesis with the observed spatial and temporal patterns of temperature change have been pointed out by T. R. Karl, R. W. Knight, G. Kukla, and J. Gavin [in *Aerosol Forcing of Climate*, R. J. Charlson and J. Heintzenberg, Eds. (Wiley, Chichester, UK, 1995), pp. 363–382].
5. D.-Z. Sun and Z. Liu, *Science* **272**, 1148 (1996).
6. J. D. Neelin and H. A. Dijkstra, *J. Clim.* **8**, 1325 (1995); H. A. Dijkstra and J. D. Neelin, *ibid.*, p. 1343.
7. A. C. Clement, R. Seager, M. A. Cane, S. E. Zebiak, *ibid.* **9**, 2190 (1996).
8. M. Latif, R. Kleemon, C. Eckert, in preparation.
9. J. Bjerknes, *Mon. Weather Rev.* **97**, 163 (1969).
10. M. A. Cane, in *Teleconnections Linking Worldwide Climate Anomalies*, M. Glantz, R. W. Katz, N. Nicholls, Eds. (Cambridge Univ. Press, Cambridge, 1991), pp. 345–369.
11. The thermocline is a region of sharp temperature change separating the warm surface layers from the cold abyssal waters.
12. S. E. Zebiak and M. A. Cane, *Mon. Weather Rev.* **115**, 2262 (1987). Details of the calculations used to produce Fig. 1 are described in (*7*). The model domain is 29°S to 29°N, 124°E to 80°W.
13. J. McCreary and P. Lu, *J. Phys. Oceanogr.* **24**, 466 (1994); Z. Liu, S. G. H. Philander, R. Pacanowski, *ibid.*, p. 1606.
14. J. R.. Toggweiler, K. Dixon, W. S. Broecker, *J. Geophys. Res.* **96**, 20467 (1991).
15. R. Seager and R. Murtugudde, *J. Clim.*, in press.
16. T. R. Knutson and S. Manabe, *ibid.* **8**, 2181 (1995).
17. S. Tett, *ibid.*, p. 1473.
18. G. A.. Meehl and W. M. Washington [*Nature* **382**, 56 (1996)] provide an alternative mechanism for greater east Pacific warming. Following V. Ramanathan and W. D. Collins [*ibid.* **351**, 27 (1991)], they assumed that the albedo of deep convective clouds increases with SST. As the climate warms, this larger albedo reduces the solar radiation absorbed in the west Pacific relative to that in the east. This cirrus cloud thermostat mechanism has been criticized by some [see, for example, R. Fu, A. D. DelGenio, W. B. Rossow, W. T. Liu, *ibid.* **358**, 394 (1992); D. Hartmann and M. Michelson, *J. Clim.* **6**, 2049 (1993); R. T. Pierrehumbert, *J. Atmos. Sci.* **52**, 1784 (1995)].
19. "Coupling" is used in the ENSO literature to mean a feedback loop wherein a given change in SST causes a change in equatorial wind stress that results in a change in thermocline depth and finally SST. The ratio of the final to initial SST change would be a measure of "coupling" strength. Note that the oceanic changes are dynamical. Thermodynamics enters the loop only through its effect on wind stress.
20. N. C. Lau, S. G. H. Philander, M. J. Nath, *J. Clim.* **5**, 284 (1992); S. Manabe and R. J. Stouffer, *ibid.* **9**, 376 (1996); J. D. Neelin *et al.*, *Clim. Dyn.* **7**, 73 (1992).
21. A. Kaplan *et al.* (in preparation) present a global analysis and validation. The method [developed by A. Kaplan, M. A. Cane, Y. Kushnir, and B. Blumenthal (in preparation)] uses empirically derived time and space covariance estimates to obtain an optimally smoothed analysis of Atlantic SSTs from 1856 to 1991. The analysis procedure is similar to so-called "optimal interpolation" in that it uses estimates of spatial covariance to fill gaps in the data. In addition, it makes limited use of temporal covariance estimates in a Kalman Smoother algorithm; the SST data comes from (*27*).
22. Although the analysis extends from 1856 to 1991, we went back no further than 1900 because of suspicions that the 19th-century SSTs are systematically in error (*1*, *20*).
23. The Lamont model has a well-known bias that places the maximum SST anomaly too far east; allowing for this would further increase the resemblance of Fig. 1 to the observed pattern.
24. K. Trenberth and T. Hoar, *Geophys. Res. Lett.* **23**, 57 (1996).
25. B. Rajagopalan, U. Lall, M. A. Cane, in preparation.
26. The global pattern correlation between Fig. 3, A and B, is 0.97. We also computed the first empirical orthogonal function of the data with ENSO removed; its principal component is largely trend and correlates with the trend patterns at 0.95 or more.
27. M. Bottomley, C. K. Folland, J. Hsiung, R. E. Newell, D. E. Parker, *Global Ocean Surface Temperature Atlas (GOSTA)* (Her Majesty's Stationary Office, London, 1990). This atlas is based on the U.K. Meteorological Office Main Marine Data Bank and includes corrections for systematic measurement errors. The version of the GOSTA data set that was used in (*21*), MOHSST5 [D. E. Parker *et al.*, in *Natural Climate Variability on Decade to Century Timescales* (National Academy Press, Washington, DC, 1996), pp. 244–250], incorporates COADS (*28*) values where GOSTA data are deficient and uses an improved scheme of corrections for instrumental biases [C. K. Folland and D. E. Parker, *Q. J. R. Meteorol. Soc.* **121**, 319 (1995)].
28. S. D. Woodruff, R. J. Slutz, R. L. Jenue, P. N. Steurer, *Bull. Am. Meteorol. Soc.* **68**, 521 (1987).
29. Trends and confidence limits are based on a median estimator, the Sens slope test [see, for example, R. O. Gilbert, *Statistical Methods for Environmental Pollution Monitoring* (Van Nostrand Reinhold, New York, 1987)]. The more commonly used least squares trend estimates are less robust. The least squares trend estimates are (in degrees Celsius per century, with 95% confidence limits) $+0.72 \pm 0.63$ for the analysis, $+0.22 \pm 0.69$ for GOSTA, and $+0.35 \pm 0.62$ for COADS.
30. For a recent review with many references, see N. C. Lau, *Bull. Am. Meteorol. Soc.*, in press.
31. E. K. Schneider, B. Kirtman, R. S. Lindzen, *J. Clim.*, in press.

4 October 1996; accepted 27 December 1996

Potential Involvement of Fas and Its Ligand in the Pathogenesis of Hashimoto's Thyroiditis

Carla Giordano,* Giorgio Stassi,* Ruggero De Maria,* Matilde Todaro, Pierina Richiusa, Giuliana Papoff, Giovina Ruberti, Marcello Bagnasco, Roberto Testi,† Aldo Galluzzo

The mechanisms responsible for thyrocyte destruction in Hashimoto's thyroiditis (HT) are poorly understood. Thyrocytes from HT glands, but not from nonautoimmune thyroids, expressed Fas. Interleukin-1β (IL-1β), abundantly produced in HT glands, induced Fas expression in normal thyrocytes, and cross-linking of Fas resulted in massive thyrocyte apoptosis. The ligand for Fas (FasL) was shown to be constitutively expressed both in normal and HT thyrocytes and was able to kill Fas-sensitive targets. Exposure to IL-1β induced thyrocyte apoptosis, which was prevented by antibodies that block Fas, suggesting that IL-1β–induced Fas expression serves as a limiting factor for thyrocyte destruction. Thus, Fas-FasL interactions among HT thyrocytes may contribute to clinical hypothyroidism.

The interaction of Fas (CD95/APO-1) with its ligand (FasL) regulates a number of physiological and pathological processes of cell death. Triggering of Fas contributes to the regulation of the immune response and tissue homeostasis, as well as to the immunological clearance of virus or tumor cells (*1*).

Hashimoto's thyroiditis (HT) is an autoimmune disorder in which destructive processes overcome the potential capacity of thyroid replacement, estimated as about 5- to 10-fold in a lifetime (*2*). Apoptosis has been occasionally observed in histological section of normal thyroid (*3*). However, apoptotic cell death is abnormally accelerated during the pathologic phases leading to clinical hypothyroidism (*4*).

The mechanisms responsible for thyrocyte destruction remain elusive (*5*). Normal thyrocytes do not express Fas (*6*). However, Fas is inducible in some cell types upon appropriate stimulation (*1*). To determine the possible involvement of Fas and its ligand in autoimmune thyroid destruction, we first analyzed Fas expression in thyroid specimens from active HT and from nontoxic goiter (NTG) patients. Immunohistochemistry of frozen thyroid sections and two-color flow cytometric analysis of dispersed thyroid follicular cells, obtained by enzymatic digestion, revealed that HT thyrocytes, identified for cytokeratin (Fig. 1A) and thyroperoxi-

C. Giordano, G. Stassi, M. Todaro, P. Richiusa, A. Galluzzo, Laboratory of Immunology, Endocrinology Section, Institute of Clinica Medica, University of Palermo, Palermo, Italy.
R. De Maria and R. Testi, Department of Experimental Medicine and Biochemical Sciences, University of Rome "Tor Vergata," Rome, Italy.
G. Papoff and G. Ruberti, Department of Immunobiology, Institute of Cell Biology, CNR, Rome, Italy.
M. Bagnasco, Allergology and Clinical Immunology, University of Genova, Genoa, Italy.

*These authors contributed equally to this work.
†To whom correspondence should be addressed. E-mail: tesrob@flashnet.it

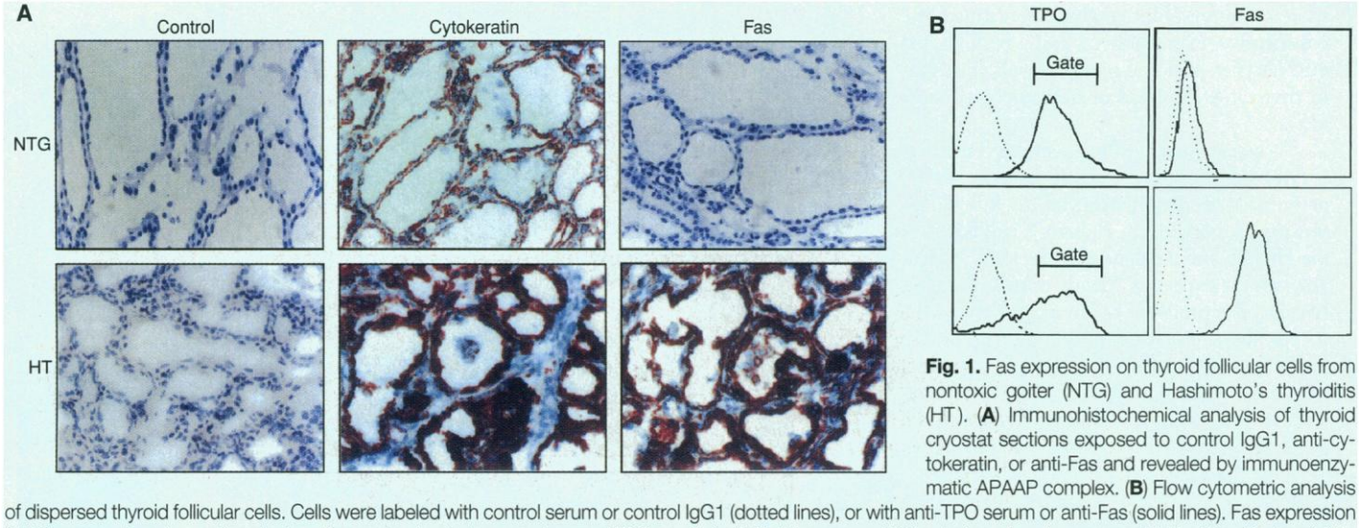

Fig. 1. Fas expression on thyroid follicular cells from nontoxic goiter (NTG) and Hashimoto's thyroiditis (HT). (**A**) Immunohistochemical analysis of thyroid cryostat sections exposed to control IgG1, anti-cytokeratin, or anti-Fas and revealed by immunoenzymatic APAAP complex. (**B**) Flow cytometric analysis of dispersed thyroid follicular cells. Cells were labeled with control serum or control IgG1 (dotted lines), or with anti-TPO serum or anti-Fas (solid lines). Fas expression (right) was analyzed on cells gated on thyrocyte physical parameters and TPO positivity (left). (Upper panels) Nontoxic goiter. (Lower panels) Hashimoti's thyroiditis.

dase (TPO) positivity (Fig 1B), express large amounts of Fas on their cell surface (*7*).

The expression of Fas in thyrocytes from HT patients may be a consequence of the intense inflammatory process. We therefore examined whether the exposure of normal thyrocytes to inflammatory cytokines could induce Fas expression in vitro. IL-1β was the only cytokine, among those found in HT glands (*8*), able to induce Fas expression in normal thyrocytes (Fig. 2A). Other cytokines, such as tumor necrosis factor–α (TNF-α), interferon-γ (IFN-γ), IL-6, and IL-12, failed to promote Fas expression (Fig. 2A). IL-1β–induced Fas expression was detectable at doses as low as 5 U/ml, reaching high levels at concentrations around 100 U/ml (Fig. 2, B and C). Both cycloheximide and actinomycin D completely prevented IL-1β–induced thyrocyte Fas expression (Fig. 2B), indicating that new RNA and protein synthesis is required in this process. As expected, IL-1β was abundantly present in HT tissue (Fig. 2, D and E).

These results were suggestive for a role of Fas in thyrocyte destruction. Because Fas expression does not always correlate with its apoptotic function (*9*), we examined whether Fas was able to transduce a death signal in thyrocytes. Triggering of Fas, after its in vitro induction by IL-1β on normal thyrocytes, resulted in massive apoptotic cell death, indicating that Fas is functional and induces apoptosis in thyrocytes (Fig. 3, A and C). Moreover, IL-1β–induced Fas expression resulted in appreciable thyrocyte apoptosis, in a dose-dependent fashion (Fig. 3, A to C). Importantly, immunohistochemical analysis of HT thyroid specimens revealed several apoptotic cells among the Fas-positive thyrocytes (Fig. 3D). By contrast, Fas-negative NTG thyrocytes did not show any sign of apoptosis (Fig. 3D) (*10*).

FasL expression by activated lymphocytes dictates the fate of activated Fas-sensitive lymphocytes (*11*). However, FasL expression is not confined to the immune system, as mouse eye and testis produce high levels of this cytokine (*12*). Moreover, FasL expression has been detected in hepatocytes from patients with alcoholic liver damage (*13*). We therefore investigated whether FasL was expressed in HT and nonautoimmune thyroid glands. Unexpectedly, FasL was constitutively expressed on both nonautoimmune and HT thyrocytes, as demonstrated by immunohistochemical analysis of frozen sections (Fig. 4A) and by two-color flow cytometric analysis of dispersed TPO-positive thyrocytes (Fig. 4B) (*14*). Accordingly, reverse transcriptase–polymerase chain reaction (RT-PCR) analysis performed on mRNA isolated from NTG or HT glands revealed that FasL mRNA was present in both autoimmune or nonautoimmune conditions (Fig. 4C) (*15*). FasL expression by HT thyrocytes was abundant (Fig. 4B), about four- or fivefold higher than that found on the small percentage of FasL-positive lymphocytes infiltrating HT glands (*16*). The presence of FasL was further investigated on purified normal thyrocytes. RT-PCR and

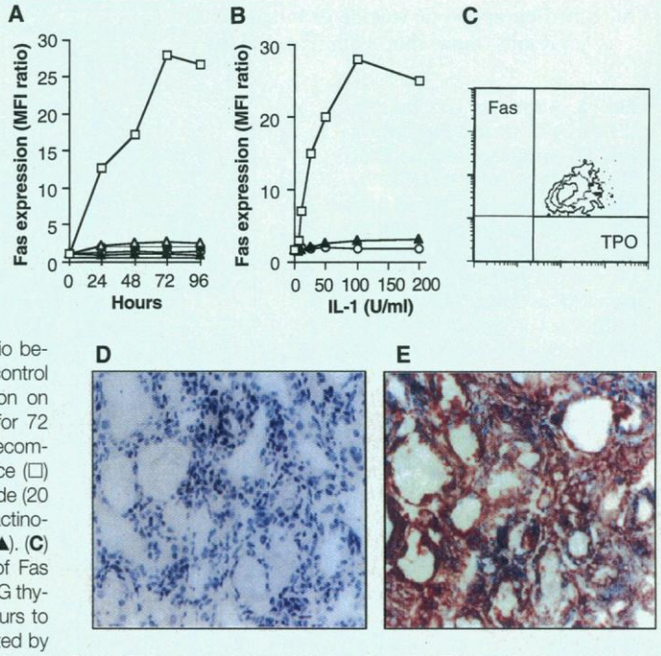

Fig. 2. Fas expression on normal thyrocytes induced by exposure to IL-1β. (**A**) Kinetics of Fas expression on NTG thyrocytes exposed to recombinant IL-1β (200 U/ml; Genzyme) (□), IL-6 (Genzyme) (■), TNF-α (Boehringer GmbH, Mannheim, Germany) (○), IL-12 (Genzyme) (▲), and IFN-γ (Sigma) (△). Data are presented as mean fluorescence intensity (MFI) ratio (the ratio between MFI of specific and control staining). (**B**) Fas expression on NTG thyrocytes exposed for 72 hours to various doses of recombinant IL-1β, in the absence (□) or presence of cycloheximide (20 μg/ml; Sigma) (○) or with actinomycin D (5 μg/ml; Sigma) (▲). (**C**) Simultaneous expression of Fas expression and TPO on NTG thyrocytes exposed for 72 hours to IL-1β (100 U/ml), as detected by two-color flow cytometric analysis. (**D** and **E**) Immunohistochemical analysis of HT thyroid cryostat sections exposed to control IgG1 (D) or IL-1β mAb (E) and revealed by immunoenzymatic APAAP complex procedure. Anti–IL-1β (IgG1) was from Genzyme, and secondary and immunoenzymatic reagents were from Dakopatts.

protein immunoblot analysis confirmed the constitutive expression of FasL, both at the mRNA (Fig. 4D) and protein levels (Fig. 4E), in thyrocytes depleted of hematopoietic cells (*15*).

To assess whether FasL expressed on thyrocytes is functional, we compared the ability of purified normal thyrocytes to kill a Fas-sensitive subline of the human T cell lymphoma HuT78 and a Fas-insensitive HuT78 variant, which expresses "death domain"–defective Fas receptors (*17*). Thyrocytes were able to lyse Fas-sensitive but not Fas-insensitive HuT78 cells (Fig. 5A). Moreover, cytotoxicity against Fas-sensitive HuT78 was completely prevented by the addition of monoclonal antibodies (mAbs) blocking Fas (*18*) (Fig. 5A), demonstrating that FasL on thyrocytes is able to induce apoptotic cell death through the engagement of functional Fas.

Normal thyrocytes do not undergo apoptosis, because they express negligible amounts of Fas. However, simultaneous expression of functional Fas and FasL in HT or in IL-1β–stimulated thyrocytes might result in apoptotic cell death. To address this hypothesis, we examined whether IL-1β–induced apoptosis could be blocked by interfering with Fas-FasL interactions. As shown by flow cytometry of propidium iodide (PI)–labeled thyrocytes and ethidium bromide–acridine orange staining and fluorescence microscopy analysis, the addition of mAbs that block Fas completely suppressed IL-1β–induced apoptotic cell death in vitro (Fig. 5, B and C). These findings demonstrated that IL-1β–mediated induction of Fas on thyrocytes, which constitutively express FasL, results in their apoptotic suicide or fratricide.

Our results show that both Fas and its

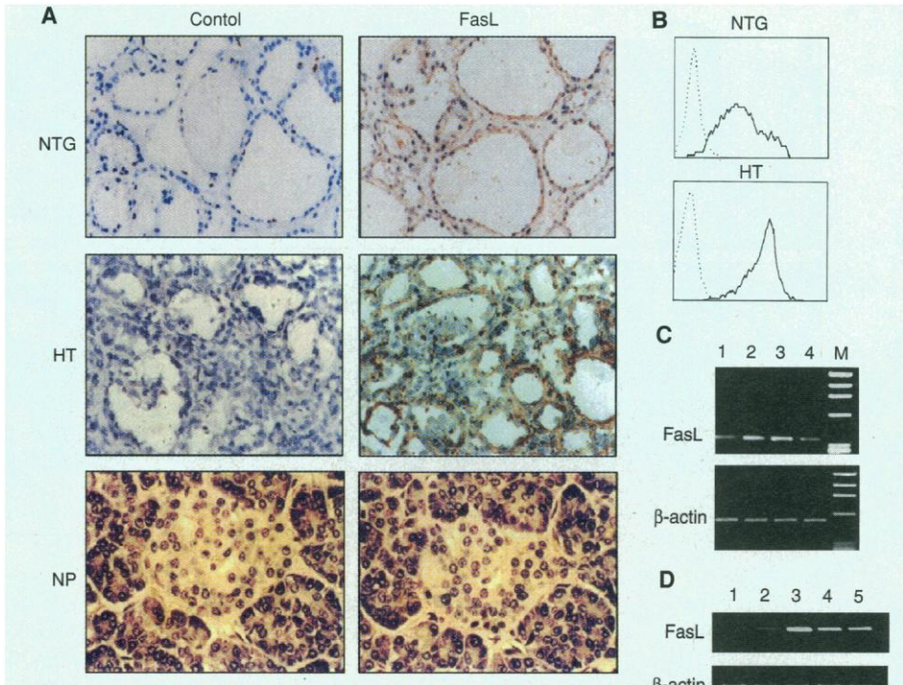

Fig. 4. Constitutive expression of FasL by thyrocytes. (**A**) Immunohistochemical analysis of NTG, HT thyroid, or normal pancreatic (NP) cryostat sections exposed to control rabbit IgG or rabbit anti-FasL and visualized by immunoperoxidase. (**B**) Flow cytometric analysis of dispersed TPO-positive thyrocytes. Cells were labeled with anti-FasL (solid lines) or control IgG (dotted lines). (**C**) RT-PCR in thyroid tissues. Lanes 1 and 2, samples of NTG tissues from two different individuals; lanes 3 and 4, samples from two different HT patients. ϕ X174 DNA–Hae III digest was used as a size marker (M). (**D**) RT-PCR in normal human pancreatic islets (lane 1), Jurkat (human T cell leukemia) cells (lane 2), Jurkat cells activated with phorbol 12-myristate 13-acetate (PMA, 10 ng/ml) and ionomycin (400 ng/ml) for 4 hours (lane 3), normal thyroid tissue (lane 4), or hematopoietic cell–depleted thyrocytes (lane 5). (**E**) Immunoblot detection of FasL on cell lysates from Jurkat cells (lane 1), Jurkat cells activated with PMA (10 ng/ml) and ionomycin (400 ng/ml) for 4 hours (lane 2), normal thyroid tissue (lane 3), or hematopoietic cell–depleted thyrocytes (lane 4). FasL was visualized by staining with anti-FasL and the ECL detection system. Molecular sizes are indicated on the right (in kilodaltons).

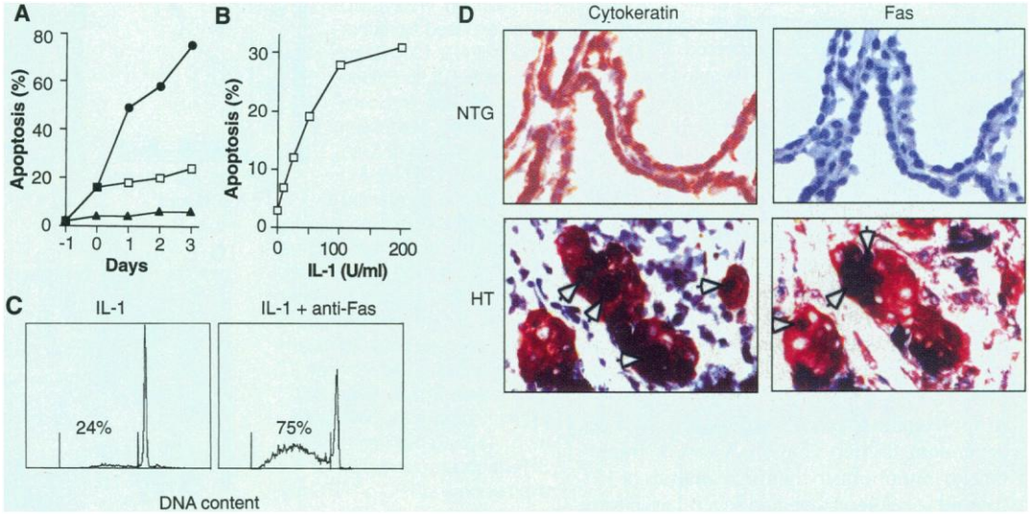

Fig. 3. Thyrocyte apoptosis induced by IL-1β and Fas stimulation. (**A**) Percentage of hypodiploid nuclei of freshly separated NTG thyrocytes cultivated for various times with medium alone (▲) or with the addition of recombinant IL-1β (50 U/ml) at day −1, and anti-Fas (200 ng/ml) (●) or control IgM (□) at day 0. (**B**) Effect of 36-hour exposure of NTG thyrocytes to various doses of IL-1β. (**C**) Flow cytometric profiles of DNA content of nuclei from NTG thyrocytes exposed for 72 hours to IL-1β and IL-1β plus anti-Fas. CH-11 (anti-Fas IgM) was from Upstate Biotechnology (New York, New York). The percentage of hypodiploid nuclei was determined by hypotonic fluorochrome solution staining (50 μg of PI per milliliter in 0.1% sodium citrate plus 0.1% Triton X-100) (Sigma) and flow cytometric analysis, as described (*9*). (**D**) Detection of in situ DNA breaks by terminal deoxynucleotidyl transferase dUTP nick end labeling (TUNEL) and BCIP (black) staining onNTG and HT section labeled with anticytokeratin or anti-Fas, with an avidin-biotin complex and 3-amino-9-ethylcarbazole as a substrate (red). Arrowheads indicate some apoptotic nuclei among CK- and Fas-expressing cells.

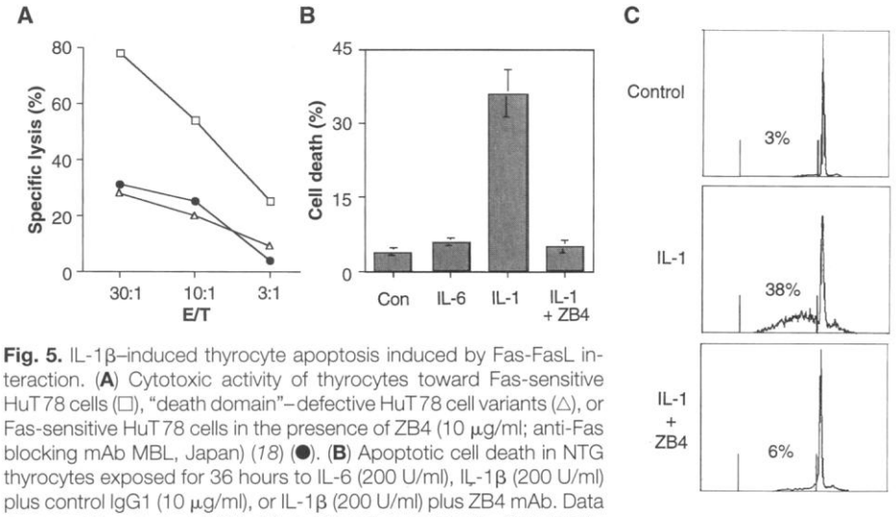

Fig. 5. IL-1β–induced thyrocyte apoptosis induced by Fas-FasL interaction. (**A**) Cytotoxic activity of thyrocytes toward Fas-sensitive HuT 78 cells (□), "death domain"–defective HuT 78 cell variants (△), or Fas-sensitive HuT 78 cells in the presence of ZB4 (10 μg/ml; anti-Fas blocking mAb MBL, Japan) (*18*) (●). (**B**) Apoptotic cell death in NTG thyrocytes exposed for 36 hours to IL-6 (200 U/ml), IL-1β (200 U/ml) plus control IgG1 (10 μg/ml), or IL-1β (200 U/ml) plus ZB4 mAb. Data represent the mean ± 1 SD of five different experiments. Cell viability was determined by orange acridine–ethidium bromide staining and fluorescence microscopy analysis. (**C**) Flow cytometric analysis of nuclei from thyrocytes treated as in (B). Hypodiploid nuclei were evaluated by PI staining and flow cytometric analysis.

ligand are present in HT glands and that their concomitant expression on thyrocytes is responsible for the induction of programmed cell death. Because FasL is constitutively expressed in normal thyroids, IL-1β–induced Fas expression may represent a critical limiting factor for the acceleration of thyrocyte destruction during the course of the inflammatory process. IL-1β, probably released by infiltrating monocytes or macrophages (or both) or by activated endothelial cells, can interact directly with thyrocytes, and thyrocyte destruction can proceed in a manner relatively independent of infiltrating T lymphocytes. Although autoreactive T lymphocytes may contribute to the HT thyroid-infiltrating cells (*19*), there is no evidence that cytotoxic T lymphocytes are directly involved in thyrocyte destruction. Attempts to localize cytotoxic T lymphocytes in situ revealed that only a few T lymphocytes, among those which infiltrate HT thyroids, contain perforin (*20*). Moreover, we found that the expression of FasL on infiltrating T lymphocytes is negligible compared to FasL expression on HT thyrocytes. These observations suggest a minor role for cytotoxic T lymphocytes and a prevailing involvement of FasL expressed by thyrocytes in tissue destruction. It is likely that this process is then further amplified by autoantibody-mediated cytotoxicity, as new antigenic determinants are exposed after initial tissue destruction.

In conclusion, we provide evidence suggesting that Fas-FasL interactions among thyrocytes may contribute to the pathogenesis of HT. Although infiltrating T lymphocytes may participate to this process, our results demonstrate that thyrocytes undergo Fas-mediated apoptosis after IL-1β exposure without the contribution of other cells. This mechanism might be operating in all forms of hypothyroidism that follow inflammation.

REFERENCES AND NOTES

1. S. Nagata and P. Golstein, *Science* **267**, 1449 (1995); P. H. Krammer *et al.*, *Immunol. Rev.* **142**, 175 (1994); K. Schulze-Osthoff, *Trends Cell Biol.* **4**, 421 (1994).
2. J. Coclet, F. Foureau, P. Ketelbant, P. Galand, J. E. Dumont, *Clin. Endocrinol.* **31**, 655 (1989); J. E. Dumont, F. Lamy, P. Roger, C. Maenhout, *Physiol Rev.* **72**, 667 (1992).
3. S. Dremier *et al. Biochem. Biophys. Res. Commun.* **200**, 52 (1994).
4. T. Kotani *et al. Autoimmunity* **20**, 231 (1995).
5. B. R. Champion, A. Cooke, D. C. Rayner, *Curr. Opin. Immunol.* **4**, 770 (1992); A. P. Weetman and A. M. McGregor, *Endocr. Rev.* **15**, 788 (1994).
6. F. Leithauser *et al.*, *Lab. Invest.* **69**, 415 (1993).
7. For immunohistochemistry, 0.5-cm fragments of thyroid tissue obtained at surgery were snap-frozen, then 4-μm sections were cut in a Miles Microtome and kept at −70°C until use. Just before staining, the sections were allowed to equilibrate to room temperature and were exposed to absolute acetone for 10 min, followed by air-drying for another 10 min. Then immunoenzymatic alkaline phosphatase antialkaline phosphatase (APAAP) complex procedure was used. Control sections were set up with irrelevant isotype-matched mAbs. Anti-cytokeratin [CK1 mAb, immunoglobulin G1 (IgG1)] was from Dakopatts (Santa Barbara, CA), and anti-Fas (UB2, IgG1) was from Kamiya Biomedical Company (Thousand Oaks, CA). For two-color flow cytometric analysis, thyroid tissue obtained at surgery was digested with collagenase type IV S (5 mg/ml; Sigma) for 2 hours at 37°C. The digest was filtered through a 200-μm mesh, and cells were plated in 75-cm^2 flasks in complete medium (RPMI 1640 supplemented with 10% fetal calf serum and glutamine). After overnight adhesion, unattached cells were discarded, whereas thyrocytes were removed from the flasks with 0.05% (w/v) trypsin. These cell preparations underwent a second digestion with dispase to obtain single-cell suspensions. Thyrocytes were then labeled with human serum containing anti-TPO, followed by labeling with fluorescein isothiocyanate–coupled goat anti-human Ig. Cells were then incubated for 10 min with 6% normal mouse serum before staining with phycoerithrin-conjugated UB2 mAb. Relative fluorescent intensities of individual cells were analyzed with a FACScan flow cytometer (Becton Dickinson).
8. B.Grubeck-Loebenstein *et al.*, *Clin. Exp. Immunol.* **77**, 324 (1989).
9. R. De Maria *et al. J. Clin. Invest.* **97**, 1 (1996).
10. Fas- or CK-labeled cryostat thyroid sections (5 μm) were fixed in paraformaldehyde, permeabilized with 0.1% Triton X-100, and labeled by an in situ apoptosis detection kit (in situ cell death detection, alkaline phosphatase; Boehringer GmbH, Mannheim, Germany). Detection of labeled ends was done with anti-fluorescein, Fab fragment, conjugated with alkaline phosphatase. 5-Bromo-4-chloro-3-indolyl phosphate (BCIP) (Dakopatts) was used as substrate. Sections were then counterstained with hematoxylin.
11. J. Dhein, H. Walczak, C. Baumler, K.-M. Debatin, P. H. Krammer, *Nature* **373**, 438 (1995); T. Brunner *et al.*, *ibid.*, p. 441.
12. D. Bellgrau *et al.*, *ibid.* **377**, 630 (1995); T. S. Griffith, T. Brunner, S. M. Fletcher, D. R., Green, T. A. Ferguson, *Science* **270**, 1189 (1995); L. A. French *et al.*, *J. Cell Biol.* **133**, 335 (1996).
13. P. R. Galle *et al.*, *J. Exp. Med.* **182**, 1223 (1995).
14. Sections were allowed to equilibrate to room temperature and were exposed to hydrogen peroxide methanol solution for 5 min. Then slides were rinsed with distilled water and placed for 5 min in a tris buffer before staining with peroxidase-antiperoxidase. Control sections were exposed with control purified rabbit IgG. Anti-FasL (C-20, rabbit polyclonal IgG) was from Santa Cruz Biotechnology (Santa Cruz, CA). For flow cytometric analysis, freshly purified thyrocytes were treated with C-20 or control rabbit IgG, followed by phycoerithrin-conjugated goat anti-rabbit IgG (Sigma), as secondary reagent.
15. For RT-PCR, RNA from cells or homogenized tissues was prepared by guanidine isothiocyanate–acid phenol extraction. Two micrograms of total RNA were used in a first-strand cDNA synthesis with random examer oligonucleotides and amplified by PCR, generating a 345–base pair (bp) fragment of human FasL (forward primer: 5′-CAAGTCCAACTCAAGGTCCATGCC-3′; reverse primer: 5′-CAGAGAGAGCTCAGATACGTTTGAC-3′) or a 518-bp fragment of human β-actin (forward primer: 5′-TCGTCGACAACGGCTCCGGCATGT-3′; reverse primer: 5′-CCAGCCAGGTCCAGACGCAGGAT). The RT-PCR products were subjected to electrophoresis on a 2% agarose gel and stained with ethidium bromide. For protein immunoblots, proteins were isolated from 20×10^6 cells with the TRIzol reagent (Gibco-BRL). An equal amount of proteins (100 μg) was resolved by 10% SDS–polyacrylamide gel electrophoresis under reducing conditions and transferred to nitrocellulose. FasL was detected with anti-FasL (Clone 33; Transduction Laboratories, Lexington, KY), followed by anti-mouse horseradish peroxidase and the ECL detection system (Amersham, Bucks, UK). For immunodepletion of contaminating hematopoietic cells, thyrocyte single-cell suspensions were treated with anti-CD45 (Anti-Leukocyte, Becton Dickinson) for 30 min at 4°C. CD45$^+$ cells were then removed after 30 min binding to sheep anti-mouse IgG-coupled beads (Dynal, Wirral Merseyside, UK) and magnetic depletion.
16. C. Giordano *et al.*, data not shown.
17. M.G. Cifone *et al.*, *EMBO J.* **14**, 5859 (1995); I. Cascino, G. Papoff, R. De Maria, R. Testi, G. Ruberti, *J. Immunol.* **156**, 13 (1996).
18. W. C. Liles, P. A. Kiener, J. A. Ledbetter, A. Aruffo, S. J. Klebanoff, *J. Exp. Med.* **184**, 429 (1996). Target cells were incubated overnight with 1 μM 3,3′-dioctadecyloxacarbocyanine and exposed for 6 hours to various amounts of purified thyrocytes. Then target lysis was measured by flow cytometric analysis with the LIVE/DEAD, cell-mediated cytotoxicity kit (Molecular Probes).
19. T. F. Davies *et al.*, *J. Clin. Invest.* **89**, 157 (1992).
20. Z. Wu, E. R. Podack, J. M. McKenzie, K. J. Olsen, M. Zakarija, *Clin. Exp. Immunol.* **98**, 470 (1994).

21. Supported by Associazone Italiana Ricerca sul Cancro, Telethon, Consiglio Nazionale delle Ricerche, and the European Commission. We thank P. Bazan and G. Di Pace (Department of Surgery, University of Palermo) for surgical specimens and Genzyme Diagnostic (Cambridge, UK) for IL-1.

27 June 1996; accepted 2 January 1997